Mon. Not. R. astr. Soc. (1991) **251**, 199–202

Atmospheric transmission at submillimetre wavelengths from Mauna Kea

David A. Naylor,[1] T. Alan Clark,[2] Arvid A. Schultz[1] and Gary R. Davis[3]

[1] *University of Lethbridge, Department of Physics, Lethbridge, Alberta, Canada T1K 3M4*
[2] *University of Calgary, Department of Physics and Astronomy, Calgary, Alberta, Canada T2N 1N4*
[3] *Mullard Space Science Laboratory, University College London, Holmbury St Mary, Dorking, Surrey RH5 6NT*

Accepted 1991 January 11. Received 1990 December 7; in original form 1990 June 13

SUMMARY

Measurements of the submillimetre solar spectrum through the 350- and 450-μm windows of the atmosphere using a Michelson interferometer on the James Clerk Maxwell Telescope have been used to determine the transmission spectrum of the atmosphere above Mauna Kea, Hawaii. This spectrum is shown to be in close agreement with that generated by the FASCOD synthesis program using the HITRAN database. The majority of absorption features can be attributed to H_2O (which dominates the overall window shape), O_2 and O_3, although several significant but so far unassigned absorption features are noted. These results demonstrate the feasibility, under drier and more stable atmospheric conditions, of obtaining broad-band, intermediate resolution spectra from the JCMT with a Fourier spectrometer.

1 INTRODUCTION

The 15-m James Clerk Maxwell Telescope (JCMT), located at an altitude of 4084 m near the summit of Mauna Kea, Hawaii, provides astronomers with an unprecedented opportunity to carry out observations at relatively high angular resolutions (8–10 arcsec) in the partially transparent submillimetre atmospheric windows at 350 and 450 μm. Although the transmission of the atmosphere in these windows is rarely greater than 50 per cent even under the driest conditions, the potential astronomical return is significant. The specific interests of this study were planetary and solar spectroscopic observations. In the initial phase of the study, it was decided to investigate the detailed spectral characteristics of these windows by observing the solar spectrum through a range of atmospheric airmasses using a broadband Fourier transform spectrometer on the JCMT for the first time.

2 OBSERVATIONS

The spectra presented here were obtained with a high resolution (0.01 cm^{-1}) infrared Fourier transform spectrometer (Naylor & Clark 1986), modified to operate at the $f/35$ Nasmyth focus of the JCMT using the broad-band bolometric detector UKT14 (Duncan *et al.* 1990). The characteristics of the interferometer are listed in Table 1. The interferometer was operated in the rapid-scan mode, producing a range of modulation frequencies at the detector of 20–30 Hz. This internal modulation and ac coupling from the detector to the electronics removed the requirement for chopping at or before the instrument. Two 8-hr solar observing shifts on 1990 February 4 and 5 produced over 500 individual interferograms, of which roughly half were taken at high elevation angles ($\geqslant 50°$) and were of sufficient quality to be included in the present analysis. Equivalent runs on Jupiter and the Moon were made under less favourable conditions of low and variable atmospheric transmission, and yielded poor spectra which have not been included in the present study.

3 DATA PROCESSING

In the rapid-scan mode of operation one interferogram was produced every minute. Groups of 10 interferograms taken on the Sun were followed by an equivalent group of 10 background interferograms taken on a neighbouring sky position

Table 1. Instrument characteristics.

Instrument Characteristics	
Interferometer	Single beam, rapid scan
Spectral Bands	350 and 450 μm
Resolution	0.01 cm^{-1}
Beamsplitter	Mylar, 50 μm
Detector	UKT14, 0.3K bolometer
UKT14 Aperture	27mm
Beam Width (FWHM)	~ 10 arc seconds

having the same airmass value, the whole sequence taking about 20 min. Standard Fourier transform spectroscopic analysis techniques were applied to these data. Since the optical elements in the spectrometer and detector produced negligible dispersion over the narrow spectral range of interest, a linear phase correction, determined from phase values at positions in the spectrum showing little absorption, was applied before Fourier transformation. This Fourier analysis successfully removed the 60 Hz interference that was apparent in the recorded interferograms.

The atmospheric transmission was ~10 per cent during these runs, and so each solar spectrum included a large atmospheric emission component. The average background spectrum in each group of measurements was subtracted from the average solar spectrum to produce a corrected solar spectrum. Slight differences in equivalent airmass values for solar and background spectra may have produced some of the observed variation in solar signal over relatively long time-scales, and future operational modes will be modified to reduce these effects.

4 TRANSMISSION SPECTRA

The corrected solar spectra described above were grouped according to airmass value and again co-added to produce the final spectra. Figs 1 and 2 show examples of these final spectra in the 350 μm (26–30 cm^{-1}) and 450 μm (20–24 cm^{-1}) windows, respectively, and contain data taken at airmass values in the range 1.23–1.39. The data in Fig. 1 were obtained on 1990 February 4 and have an average airmass of 1.32; those in Fig. 2, on 1990 February 5, have an average airmass of 1.28.

Observations of the Moon proved to be difficult because of its phase at the time of the observations. It has therefore not been possible to flux-calibrate the spectra, nor to remove a small amplitude ripple (~3 per cent) from the spectra caused by channel fringes generated in a plane-parallel cavity within the detector optics.

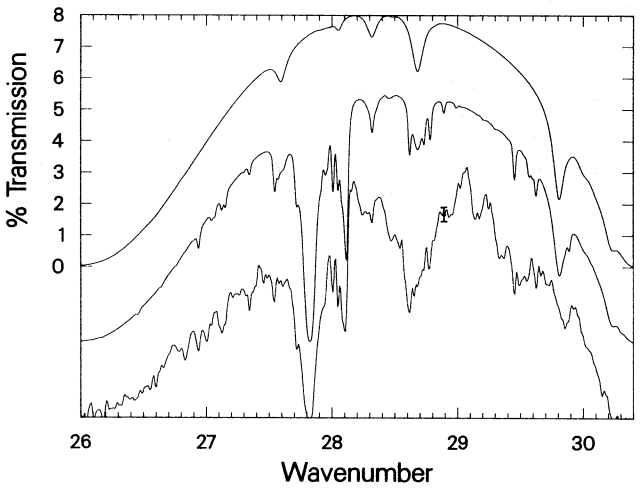

Figure 1. Transmission in 350-μm window: synthesis due to water vapour only (top trace), synthesis due to 6 major absorbers (middle trace), measured solar spectrum (bottom trace). The error bar indicates the estimated noise level per spectral element on these data.

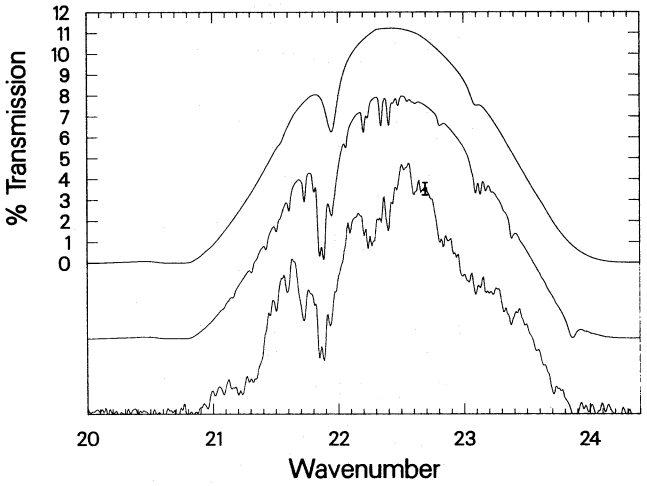

Figure 2. Transmission in 450-μm window: synthesis due to water vapour only (top trace), synthesis due to 6 major absorbers (middle trace), measured solar spectrum (bottom trace). The error bar indicates the estimated noise level per spectral element on these data.

Since this was the first time a Fourier spectrometer had been used on the JCMT, our *a priori* estimate of the noise level had large uncertainty. The signal-to-noise ratio of these spectra is estimated from a comparison of two separate subaverages of solar spectra to be ~40 per spectral resolution element (0.01 cm^{-1}). Since each average spectrum represents the difference between approximately 50 source and 50 background spectra, the noise level per individual spectrum, per spectral resolution element, per minute would then be about 6. The theoretical performance of the spectrometer can be calculated by taking into account the quoted noise level of UKT14 under typical atmospheric condition (NEFD > 10 Jy/$\sqrt{\text{Hz}}$ at 350 μm, Duncan *et al.* 1990), the efficiency of the interferometer (estimated to be ~10 per cent), and the low transmission of the atmosphere during this run (~10 per cent). Under these conditions, the power on the detector per spectral resolution element when the Sun is viewed at 350 μm with a 10 arcsec beam is $\sim 1.3 \times 10^{-12}$ W. The system NEP, given the detector noise values and the spectral bandwidths of 3 cm^{-1} (9×10^{10} Hz) is 1.6×10^{-12} W/$\sqrt{\text{Hz}}$. With these assumptions the signal-to-noise per spectral element per minute is determined to be 6.4, in excellent agreement with the measured value.

5 EXTINCTION COEFFICIENTS

Since the atmospheric attenuation is principally determined by the water vapour abundance, an estimate of the humidity in the solar line-of-sight has been obtained from a comparison of the measured extinction coefficients with those derived from synthetic modelling over a range of airmasses. In the atmospheric model described below, the main uncertainty is the validity of the term which accounts for the excess continuum absorption known to exist at these wavelengths.

The extinction coefficients have been determined for a number of selected narrow wavenumber intervals within the two windows. Representative data for two of these subwindows, 22.65–23.0 cm^{-1} and 28.4–28.5 cm^{-1}, are shown in Fig. 3. The extinction coefficients have been determined

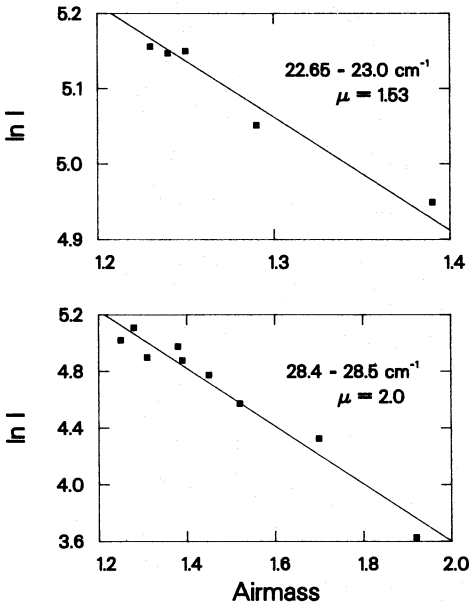

Figure 3. Plot of the intensity versus airmass in two narrow windows, from which transmission coefficients have been derived.

Table 2. Extinction coefficients in narrow sub-windows.

Feb 4th 1990

Precipitable H_2O=1.9 ± 0.1 mm in the line of sight

Wavenumber Range	Extinction Coefficient	Percentage Transmission at 1.316 airmasses
26.50 - 26.80	3.20	1.5
27.20 - 27.30	2.24	5.2
28.20 - 28.22	1.98	7.4
28.40 - 28.50	2.00	7.2
29.00 - 29.40	1.90	8.2
29.95 - 30.10	3.04	1.8

Feb 5th 1990

Precipitable H_2O=1.7 ± 0.1 mm in the line of sight

Wavenumber Range	Extinction Coefficient	Percentage Transmission at 1.28 airmasses
20.90 - 21.25	4.30	0.4
21.60 - 21.80	1.95	8.2
22.10 - 22.30	1.64	12.3
22.65 - 23.00	1.53	14.2
23.45 - 23.65	1.84	9.5

from linear fits to these data. The extinction coefficients for all of the subwindows, carefully chosen to avoid absorption lines, are listed in Table 2 along with the transmission in the line-of-sight at the average airmass.

Measurement of the extinction coefficient by observations over a range of airmasses requires that the atmospheric conditions be constant over the period of observation, which was 5 hr on February 4 for the 350 μm window and 2.25 hr on February 5 for the 450 μm window. There is some evidence in these spectra to the contrary where measurements were made at similar airmass values before and after meridian crossing of the Sun, particularly for the 350 μm window, in which intensity variations of up to 10 per cent are seen in the data at low airmass values. Some of this variation could be due to incomplete subtraction of the atmospheric spectrum, as mentioned earlier.

6 ATMOSPHERIC SIMULATION

The measured extinction coefficients have been used to derive the water vapour content of the atmosphere during these observations by comparison with a synthetic spectrum generated by the multilayer FASCOD program (Clough *et al.* 1981) utilizing the HITRAN database (Rothman *et al.* 1987) and the US standard atmosphere (1976). In addition to the principal line absorbers (H_2O, O_3, O_2, N_2O, CO and CH_4), the synthesis includes a continuum absorption term discussed by Clough *et al.* (1981). This excess absorption has been investigated at longer wavelengths by Rice & Ade (1979), and at shorter wavelengths by Davis (1987). The FASCOD continuum term has been validated on the Rice & Ade data (Anderson, private communication) and is invoked in the present analysis, but has not been verified in the 350 and 450 μm windows due to the lack of continuum measurements in these regions. Analysis of flux-calibrated spectra would provide a powerful diagnostic for the continuum absorption term at these wavelengths.

The precipitable water vapour in the line-of-sight is calculated to be 1.9 ± 0.1 mm on February 4 and 1.7 ± 0.1 mm on February 5. These correspond to zenith column abundances of 1.5 ± 0.1 and 1.3 ± 0.1 precipitable mm on February 4 and February 5, respectively. These rather high values of moisture content are probably the result of the storm which deposited a significant layer of snow upon the mountain in the days immediately preceding the observing run. Estimates of the water vapour content based on the local atmospheric conditions (relative humidity and temperature) yielded much higher values. A near-infrared absorption water vapour meter, properly calibrated against radiosonde data, would provide better estimates of the integrated water vapour content above the mountain, than can be obtained from local conditions.

The measured solar spectrum in the two submillimetre windows is compared in Figs 1 and 2 with the FASCOD synthesis. The synthesis is presented in two parts in the figures, for ease of discussion. The upper trace in each figure, and the one to which the transmission scale refers, includes only H_2O, using the water vapour abundance values determined above. The middle trace also includes O_3, O_2, N_2O, CO and CH_4, although the latter three minor constituents contribute little or no absorption in this wavelength range. The transmission of the interferometer beam-splitter and UKT14 filters and window have also been included in the calculation.

It is evident that the wings of the very broad H_2O lines combine to produce the lobe pattern of the windows, while O_3 in particular contributes much of the additional structure. The dominant absorption feature at 27.82 cm^{-1} is caused by one of the magnetic dipole transitions of molecular oxygen (Boreiko *et al.* 1984). This feature shows complete absorption at its centre but is significantly narrower than the strong

H_2O lines. There are several other absorption features in these spectra, which are considered to be significant when compared with the noise estimate discussed above. Among these are features at 22.09, 22.84 and 23.71 cm^{-1} in the 450-μm window and 26.60, 26.83, 27.01 and 27.46 cm^{-1} in the 350-μm window. Unfortunately, these features have not yet been unambiguously identified with absorption from the other minor constituents included in the HITRAN database, since many of these molecular species produce a plethora of lines across this spectral range. While these features are as yet unidentified, further measurements of such spectra, under better observing conditions, could prove useful for the identification and monitoring of these minor atmospheric species.

Thus, it is obvious that the major absorbers in these windows are H_2O and O_3 and, in view of the variability of the concentrations of these minor constituents on time-scales from minutes to days, significant variability in the window transmissions is to be expected. This will make precision photometry and spectrophotometry a challenge to even the most careful practitioners, necessitating very special and continuous cross-calibration with known and stable sources, a situation outlined by other authors (e.g. Duncan *et al.* 1990).

7 CONCLUSIONS

The present spectra, the first to be taken on the JCMT with a Fourier spectrometer operating in the rapid-scan mode, have served to highlight both the advantages and pitfalls of this approach to submillimetre solar spectroscopy from mountain sites. The overall shape of the window agrees closely with that predicted by synthetic atmospheric modelling, and the overall transmission is in reasonable agreement with the synthesis, given the assumptions used in the analysis.

The decision facing Fourier spectroscopists under these conditions as to whether to choose the rapid-scanning or step-and-integrate modes to minimize the effects of atmospheric fluctuations is a difficult one. In the former, selected in the present work, the choice is to obtain separate spectra rapidly, to average and normalize the data to remove slowly varying fluctuations in atmospheric emission and transmission and to alternate between source and background. In the latter, rapid chopping (5–10 Hz) on and off the source and narrow passband synchronous rectification will remove the majority of rapid atmospheric emission (but not transmission) fluctuations, but spectra are taken much more slowly and variations in transmission can adversely affect the spectral quality. The two-beam polarizing interferometer (Martin & Puplett 1970), with double input and output ports, has been used successfully in many applications and offers several advantages, particularly a high modulation efficiency over a wide spectral range and an absolute knowledge of the radiation paths to the detector.

The next series of measurements will use a polarizing interferometer with the option of being able to switch between rapid-scan and step-and-integrate modes, thus allowing a direct comparison of the two methods. The extended spectral range afforded by the free standing polarizers in the polarizing interferometer, compared with the limited spectral range of the present Mylar beam-splitters, will prove extremely useful from an operational point of view. If atmospheric transmission in the 350- and 450-μm windows is poor it will be possible within minutes to change a filter within UKT14 and observe at longer wavelengths where transmission can exceed 90 per cent and is much less affected by atmospheric water vapour. The expected increase in sensitivity and efficiency should help in reaching the intended goals of solar, giant planet and galactic source spectroscopy, to the stated resolution, with this telescope.

ACKNOWLEDGMENTS

We wish to thank G. J. Tompkins for the design and construction of the data acquisition electronics and for his participation as an invaluable member of the team during these runs. It is a pleasure to acknowledge the tremendous support of the JCMT team in implementing the necessary changes at the Nasmyth focus and in preparing the UKT14 detector, and to W. D. Duncan for his assistance with the operation of the telescope during the extended morning shifts. The authors are supported by grants from NSERC Canada (DAN and TAC) and SERC UK (GRD).

REFERENCES

Boreiko, R. T., Smithson, T. L., Clark, T. A. & Weiser, H., 1984. *J. Quant. Spectrosc. Radiat. Transfer.*, **32,** 109.
Clough, S. A., Kneisys, F. X., Rothman, L. S. & Gallery, W. O., 1981. *SPIE*, **277,** 152.
Davis, G. R., 1987. *D Phil thesis*, University of Oxford.
Duncan, W. D., Robson, E. I., Ade, P. A. R., Griffin, M. J. & Sandell, G., 1990. *Mon. Not. R. astr. Soc.*, **243,** 126.
Martin, D. H. & Puplett, E. F., 1970. *Inf. Phys.*, **10,** 105.
Naylor, D. A. & Clark, T. A., 1986. *SPIE*, **627,** Inst. in Astronomy VI, 482.
Rice, D. P. & Ade, P. A. R., 1979. *Inf. Phys.*, **19,** 575.
Rothman, L. S. *et al.*, 1987. *App. Opt.*, **26,** 4058.